

Impact of modified SWAT plant growth module on modeling green and blue water resources in subtropics

Tianming Ma, and Tianxiao Ma ✉

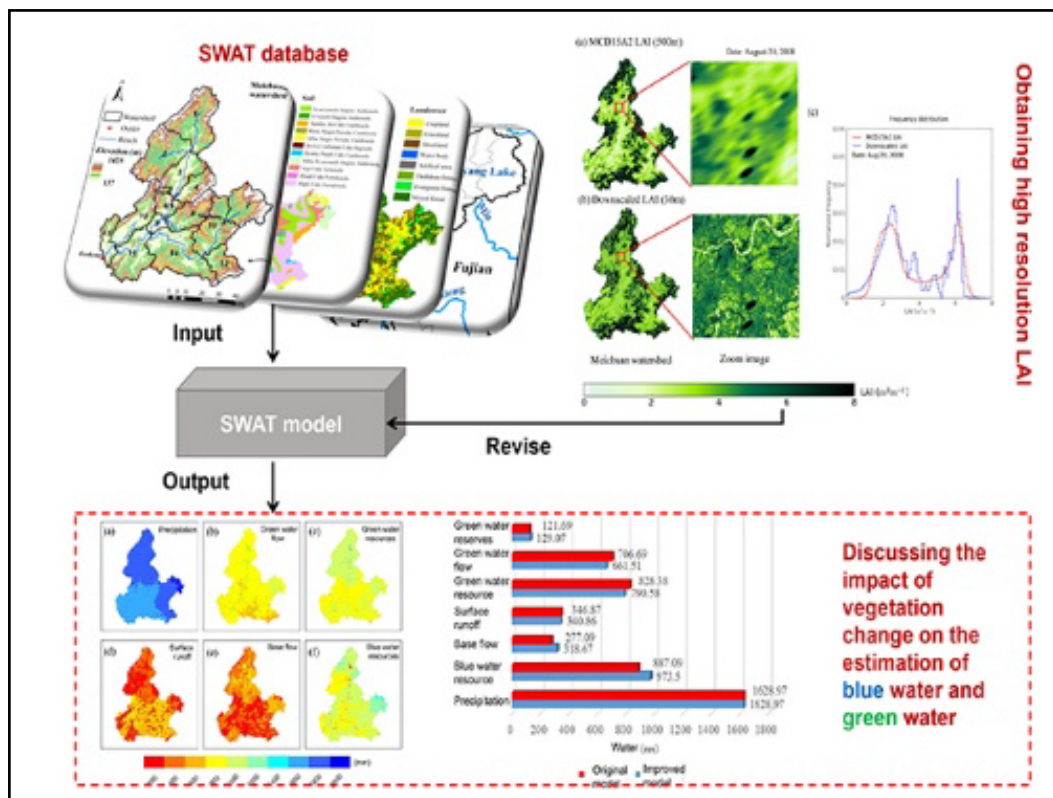
¹School of Earth and Space Sciences, University of Science and Technology of China, Hefei 230026, China;

²CAS Key Laboratory of Forest Ecology and Management, Institute of Applied Ecology, Chinese Academy of Sciences, Shenyang 110016, China

✉Correspondence: Tianxiao Ma, E-mail: matianxiao@iae.ac.cn

© 2024 The Author(s). This is an open access article under the CC BY-NC-ND 4.0 license (<http://creativecommons.org/licenses/by-nc-nd/4.0/>).

Graphical abstract




The different steps adopted to Modified SWAT Plant Growth Module on Modelling Green and Blue Water Resources in Subtropics.

Public summary


- SWAT Plant Growth Module (SWAT-EPIC) modified with remotely sensed leaf area index (LAI) has a better performance in simulations of subtropical vegetation growth.
- The modeled results using modified SWAT show that evapotranspiration is more sensitive to vegetation changes than other components of green water in a representative subtropical watershed.
- Seasonal changes of vegetation can cause a different response of blue and green water resources between forest and non-forest plant type.

Impact of modified SWAT plant growth module on modeling green and blue water resources in subtropics

Tianming Ma, and Tianxiao Ma 

¹School of Earth and Space Sciences, University of Science and Technology of China, Hefei 230026, China;

²CAS Key Laboratory of Forest Ecology and Management, Institute of Applied Ecology, Chinese Academy of Sciences, Shenyang 110016, China

 Correspondence: Tianxiao Ma, E-mail: matianxiao@iae.ac.cn

© 2024 The Author(s). This is an open access article under the CC BY-NC-ND 4.0 license (<http://creativecommons.org/licenses/by-nc-nd/4.0/>).



Cite This: *JUSTC*, 2024, 54(5): 0503 (12pp)



Read Online



Supporting Information

Abstract: The dynamics of water availability within a region can be quantitatively analyzed by partitioning the water into blue and green water resources. It is widely recognized that vegetation is one of the key factors that affect the assessment and modeling of blue and green water in hydrological models. However, SWAT-EPIC has limitations in simulating vegetation growth cycles in subtropics because it was originally designed for temperate regions and naturally based on temperature. To perform a correct and realistic assessment of changing vegetation impacts on modeling blue and water resources in the SWAT model, an approach was proposed in this study to modify the SWAT plant growth module with the remotely sensed leaf area index (LAI) to finally solve problems in simulating subtropical vegetation growth, such as controlling factors and dormancy. Comparisons between the original and modified model were performed on the model outputs to summarize the spatiotemporal changes in hydrological processes (including rainfall, runoff, evapotranspiration and soil water content) under six different plant types in a representative subtropical watershed of the Meichuan Basin, Jiangxi Province. Meanwhile, detailed analysis was conducted to discuss the effectiveness of the modified SWAT model and the impacts of vegetation changes on blue and green water modeling. The results showed that (1) the modified SWAT produced more reasonable seasonal curves of plants than the original model. E_{NS} (Nash-Sutcliffe efficiency) and R^2 increased by 0.02 during the calibration period and accounted for an increase of 0.09 and 0.03, respectively, during the validation period. (2) The comparison of model outputs between the original and modified SWAT suggested that evapotranspiration was more sensitive to vegetation changes than other components of green water. In addition, vegetation presented conservation capability in the blue water. (3) The variation in blue and green water resources with different plant types after modifying the SWAT model showed that seasonal changes in vegetation led to a significant difference between forest and non-forest areas.

Keywords: SWAT-EPIC; model applicability; subtropical regions; leaf area index; green/blue available water

CLC number: 请补充

Document code: A

1 Introduction

Blue water and green water are two basic concepts in ecological hydrology. They are also the basis and foundation of water resource evaluation^[1,2]. Blue water is the available amount of water resources, including surface rivers, lakes, reservoirs, wetlands and aquifers^[3]. Green water mainly refers to the amount of water resources related to the growth of vegetation, as explained by Falkenmark^[4]. Specifically, green water contains green water flow and green water reserves. The former mainly refers to the water content in soil (soil water volume), while the latter represents the emission of plants and the evaporation of soil and water bodies (actual evapotranspiration)^[5,6]. Water resource management has previously focused on blue water resources while ignoring green water resources^[7]. The distinction between blue water and green water provides new insight into the change in water resources. Therefore, it is of great practical significance to study the spatio-temporal changes in blue water and green

water resources to strengthen the management of water resources and solve the shortage of water resources.

The estimation methods for blue water resources currently are statistical analysis and hydrological models. For green water, its estimation methods mainly include three methods: biological models, hydrological models, and biological-hydrological coupling model^[8]. It can be easily seen that only the hydrological model can simultaneously estimate the amount of blue and green water resources and analyze the transformation between these two water resources. Vegetation is the key factor in distinguishing blue water and green water according to their definitions. It can affect rainfall, infiltration, runoff on slope and evapotranspiration processes through canopy structure in the vertical direction and community distribution in the horizontal direction, resulting in changes in land surface energy and water resources in the spatial and temporal distribution of water resources^[9-11]. Taking into account the role of vegetation, it is necessary to select hydrological models when accurately estimating the amount of blue water and green wa-

ter resources and discussing the mutual transformation mechanism between blue and green water.

The Soil and Water Assessment Tool (SWAT) model is a suitable hydrological model for evaluating the amount of blue water and green water resources under the impact of vegetation change in the watershed because this model can directly output each component of the hydrological processes by coupling several modules, such as land hydrology, vegetation cover and growth, soil erosion and nutrients^[12–13]. However, the original plant growth module of the SWAT model (EPIC plant growth model) is more applicable to simulate vegetation changes in temperate regions^[14]. When it was used to simulate vegetation growth in tropical and subtropical regions, there may be the following problems^[15]: First, the main factor controlling vegetation growth in the low-latitudes is precipitation rather than temperature; second, the dormant season in the original vegetation module of the SWAT model does not exist in these regions. These problems can cause large biases in simulating vegetation growth using the SWAT model in tropical and subtropical regions and affect the accuracy of the SWAT model in the amount and spatio-temporal distribution of blue water and green water resources.

To reduce the errors induced by the SWAT-EPIC vegetation module, we used the actual plant growth conditions from remote sensing to replace the simulated plant growth from the original module of the SWAT model in tropical and subtropical regions. The improved SWAT was applied in the Meichuan River basin, which is located in the subtropical monsoon region. By comparing the results of the SWAT model before and after improvement with the vegetation change under six different land uses, we quantitatively discussed the impact of vegetation change on the estimation and the transformation mechanism of blue water and green water. This study provides a more effective analysis tool and scientific basis for the protection, utilization and management of water resources.

2 Study area and data

The Meichuan River Basin (26°00'–27°09' N, 116°36'–116°39' E) is located in the upper reaches of the Ganjiang River Basin, covering an area of 6384 km² (Fig. 1a). As one of the main headwaters of Poyang Lake, this basin is a typical subtropical basin with a humid climate, obvious monsoon and abundant rainfall. The average annual temperature is 17°C, the annual rainfall is 1628 mm, and the average annual relative humidity is over 80%. The dominant vegetation type is subtropical evergreen forest, coniferous forest and mixed forest, covering 40.63% of the basin. Rice planting accounts for 27.19% of the basin area. In addition, there are a few shrubs and grass (Fig. 1b). The soils are mainly red soil formed by metamorphic rocks and granites and paddy soil formed by farmland cultivation. These two types of soils account for 64.3% and 28.2% of the basin area, respectively (Fig. 1c).

The research data include two parts: basic data for running the SWAT model and data for improving the SWAT model (Table 1). The soil data with a spatial resolution of 30 m were generated by the soil vector map (1 : 500,000) from the Re-

source and Environment Science and Data Center, Chinese Academy of Sciences. The Meichuan River Basin was divided into 15 sub-basins and 490 hydrological response units (HRUs) based on DEM, land use/cover, soil and other data. Runoff data from Fenheng station at the river basin output and climatic data from 6 meteorological stations and 27 precipitation stations around the study area were collected from 2001 to 2014 for model calibration and verification, respectively. MODIS leaf area index products and Landsat images are used to obtain a high spatio-temporal resolution leaf area index, which is an important input parameter and variable for improving the plant growth module of the SWAT model.

3 Methods

3.1 Limitations of the SWAT plant growth module

The original plant growth module of the SWAT model is derived from the simplified version of the EPIC model. This module assumes that the growth rate of plants is proportional to the rise in temperature. The vegetation growth can thus be modeled through the accumulated heat each day^[16]. For each type of plant, there are minimum, maximum and optimal temperatures for plant growth. Each type of plant grows when the observed temperature exceeds the minimum growth temperature (base temperature)^[17]. Each degree of daily average temperature higher than the minimum growth temperature can be counted as a heat unit (HU).

Because the SWAT-EPIC model controls vegetation growth based on HU, it is more suitable for simulations in regions with a slow accumulation of heat, i.e., temperate regions. In temperate regions, the air temperature during crop planting is approximately 10–15 °C, followed by 30–35 °C after 2–3 months. In contrast, the annual temperature in subtropical regions is higher with faster heat accumulation. Therefore, the leaf area index (LAI) that characterizes the vegetation growth status in SWAT will reach the peak quickly and remain constant for a long time^[18]. In addition, previous studies have noted that the main factor controlling vegetation growth in tropical and subtropical areas is precipitation rather than temperature^[19]. These problems suggest that the simulated vegetation growth using SWAT will produce a large bias in the subtropical zone.

The dormancy period is another factor that reduces the accuracy of SWAT simulations in tropical and subtropical basins. The term refers to a time period in which vegetation stops growing. Its duration can be calculated according to the day length and latitude^[20]. While the dormancy period for vegetation does exist in temperate regions due to its low temperature in winter, there is no duration for warmer tropical and subtropical basins throughout the year^[21].

In summary, the dormancy period and the heating accumulation associated with vegetation growth will result in significant differences when LAI simulations are produced by the SWAT model, especially in the subtropical basin. This systematic error of LAI simulation will be transferred to the other simulations of hydrological parameters, such as biomass, evapotranspiration, and soil water content, directly or indirectly reducing the estimation accuracy of green water and

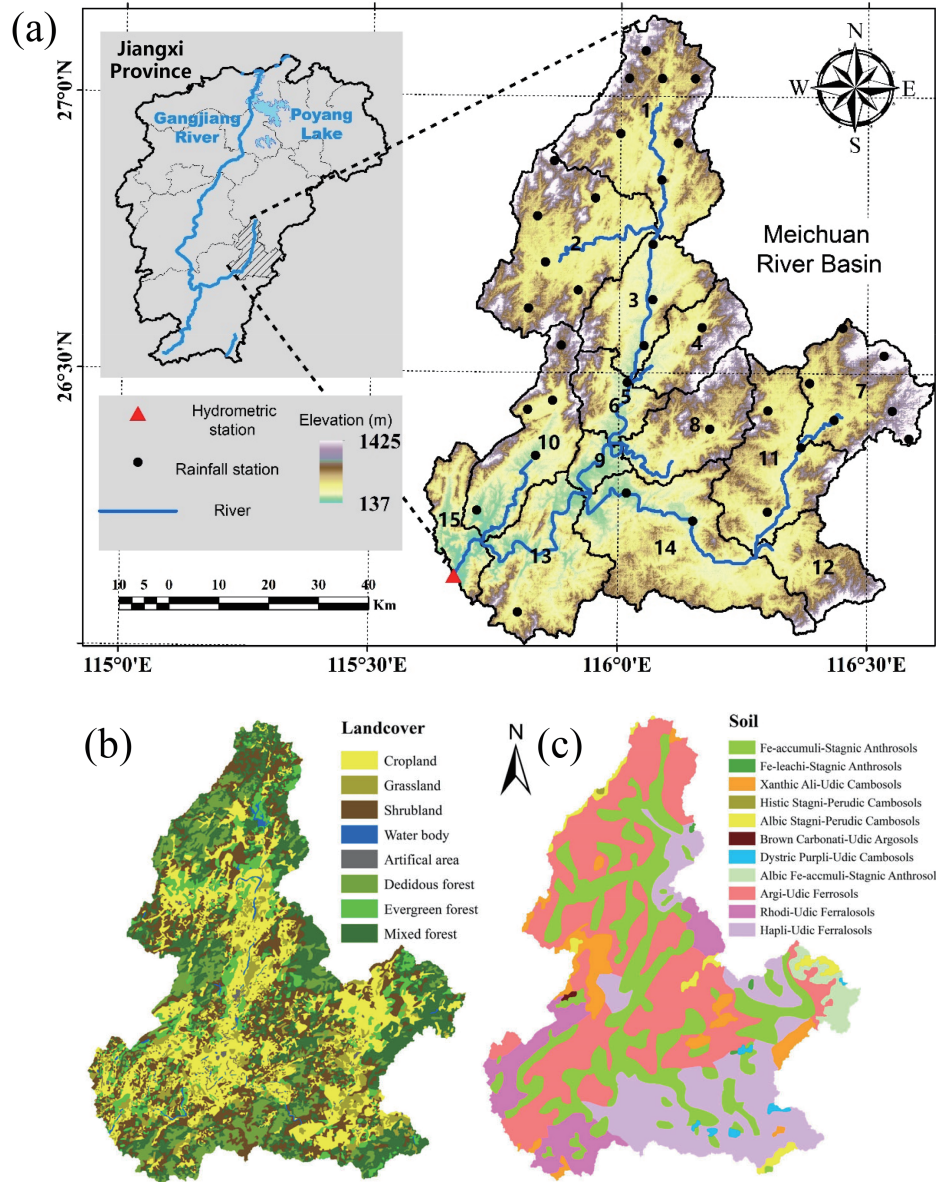


Fig. 1. (a) Locations of rain gauge stations, domain rivers, sub-basins, (b) landcover and (c) soil type in the Meichuan Basin.

Table 1. The SWAT model datasets for the Meichuan Basin.

Data type	Spatial/temporal resolution	Source
Digital elevation model	30 m	Scientific Data Center of CAS (ASTER GDEM)
Land use	30 m	Department of Earth System Science, Tsinghua University (FROM-GLC)
Soil	30 m	Resource and Environment Science and Data Center (1 : 500000)
Climate data (temperature, precipitation, wind speed, relative humidity, solar radiation)	Daily	China meteorological data service center (2001–2014)
Runoff	Daily	Hydrologic data year book (2001–2014)
Leaf area index	8 days/500 m	Scientific Data Center of CAS (MCD15A2)

blue water resources.

3.2 Improvement of the remote sensing leaf area index in the vegetation module of the SWAT model

In the vegetation module of the SWAT model, LAI represents the canopy structure and light energy utilization of the

vegetation population on the Earth’s surface. In addition, LAI is also an important parameter that affects vegetation growth^[22]. Due to the limitations in the SWAT plant growth module, the LAI simulations are not accurate in SWAT. In comparison, the dataset from remote sensing LAI can reflect the actual situation of surface vegetation. Thus, MODIS LAI

products are incorporated into the SWAT model to replace the simulated LAI of the original plant growth module. An overview of the datasets, procedures, and models is shown in the flow chart (Fig. 2). This improvement can make SWAT simulations more accurate in hydrological parameters and enhance the applicability of the SWAT model in tropical and subtropical basins.

3.2.1 High spatial and temporal resolution LAI

Due to the influence of cloud cover, sensor defects and other factors, MODIS LAI products have discontinuities in time and space^[23]. In addition, the relatively low spatial resolution (500 m) of MODIS LAI products cannot accurately depict dynamic changes in vegetation and hydrological characteristics. Therefore, it is necessary to conduct time filtering and spatial downscaling to improve the spatial and temporal resolution of data before using MODIS LAI products. The data after processing would better fit with the spatial resolution of basic data and reflect the change in LAI in the basin.

The data quality of MODIS LAI optical remote sensing products is highly susceptible to the interference of atmospheric factors such as clouds and fog in the atmosphere^[24]. Affected by these factors, LAI time series extracted from MODIS products show a sharp fluctuation. This pattern is significantly inconsistent with the reality of vegetation growth. To reduce the disturbance, the mTSF (modified temporal spatial filter) time filtering method was used in this study to smooth and reconstruct the time series of LAI data. mTSF identifies outliers for each pixel of the image by combining the quality control (QC) information contained in MODIS LAI products and uses the estimates fitted by the remote sensing data before and after multiple time periods to replace the original outliers. The processing procedures include three main steps: (1) Background calculation. The multi-year averaged LAI values of pixels with high quality were taken as

the background value. (2) Observed value calculation. The low-quality LAI values were replaced by background values in step (1), and missing values were filled by linear interpolation. (3) A final LAI value was obtained by applying a filter. Although low-quality LAI has been replaced with the multi-year averaged LAI, there are significant discontinuities in MODIS LAI products (e.g., some abnormally low LAI in the growing season). Using the results from the above steps, the adaptive Savitzky–Golay filtering method was applied to obtain a continuous and smooth LAI dynamic with final LAI values. The specific method of time filtering can be seen in reference^[25].

In the SWAT model, HRUs are the basic units for simulation. LAI, as a parameter in the plant growth module, also simulates vegetation growth based on HRU. This means that the LAI of vegetation is homogeneous in one HRU^[18]. In this study, the spatial resolution of the HRU data is 30 m, while the spatial resolution of the MODIS LAI products is 500 m. The difference between the two datasets will generate mixed pixels on the HRU boundary^[26], resulting in LAI errors in the HRU. Therefore, it is necessary to downscale MODIS LAI data to 30 m by using Landsat images with 30 m high spatial resolution to match the scale of remote sensing LAI and HRU and to depict hydrological characteristics and dynamic changes in vegetation more precisely. The Enhanced Spatial and Temporal Adaptive Reflectance Fusion Model (ESTARFM) is a spatial downscaling method that uses Landsat and MODIS surface reflectance images to downscale MODIS LAI image estimation to the scale of Landsat pixels^[27]. This method assumes that there is a linear relationship between the land surface reflectance obtained by Landsat and MODIS, which has the same physical meaning. The main steps are as follows: (1) unsupervised classification of land cover types; (2) resampling of MODIS surface reflectance and LAI data onto the Landsat pixel scale (30 m); (3) construction of the re-

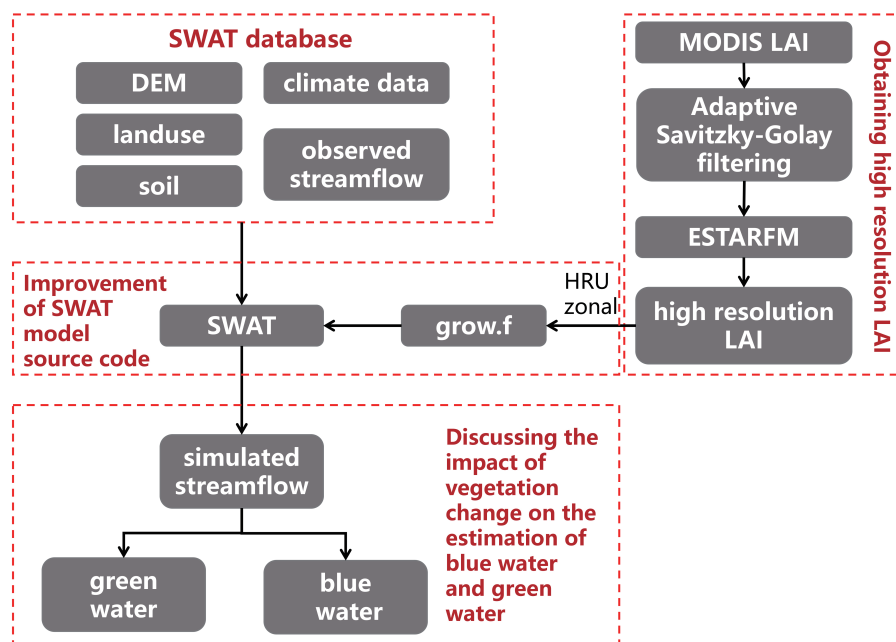


Fig. 2. Flowchart illustrating the different steps adopted to improve the SWAT plant growth module.

relationship between MODIS and Landsat surface reflectance under different land cover types; (4) application of the established surface reflectance relationship and STARFM algorithm to the initial spatial MODIS LAI products; and (5) smoothing of the downscaled LAI data to obtain the final LAI data with high spatial resolution. Detailed information for specific methods of spatial downscaling is presented in the literature^[28].

3.2.2 Improvement of SWAT model source code

The SWAT model is written in Fortran language, with a total of 306 sub-modules. Among these sub-modules, the sub-module `grow.f` is the plant growth module^[18]. Therefore, the source code related to integrated remote sensing LAI is modified in this sub-module. Since the HRU is the basic unit of SWAT model simulation, ArcGIS zonal statistics are first used to calculate MODIS LAI at the HRU level before LAI can be incorporated into the plant growth module of the SWAT model. Basically, the SWAT simulates streamflow and plant growth at a daily time step^[19]. The daily LAI was interpolated by applying a cubic spline interpolation method on each HRU using 8-day interval MODIS LAI values. These daily LAI values were defined as the input of the modified SWAT plant growth module. Then, the code for reading MODIS LAI data corresponding to each HRU is added in `grow.f` to replace the code for simulating LAI generated by the original model. Instead of LAI simulated by the plant module of the original model, MODIS LAI will directly be used to drive the model after the modification.

3.3 Model calibration and validation

The simulation periods for warm-up, parameter calibration and validation are 2001–2002, 2003–2010, and 2011–2014, respectively. In this study, the simulated results of the original model and the improved model were validated mainly through the measured runoff data at the Fenkeng hydrographic station, and the calibration of model parameters was carried out through SWAT-CUP.

SWAT-CUP is a program specially developed for automatic parameter calibration of the SWAT model. It mainly uses optimizing estimation algorithms to conduct model sensitivity tests, parameter uncertainty analysis, and automatic parameter calibration or validation^[29]. The algorithm used in this study is SUFI-2, which can randomly generate a set of parameters through the Latin hypercube sampling method to carry out the calculation of objective functions in the SWAT model^[30]. The two most commonly used objective functions are the Nash-Sutcliffe efficiency (E_{NS}) and correlation coefficient R^2 , which are expressed as follows:

$$E_{NS} = 1 - \frac{\sum_{i=1}^n (O_i - P_i)^2}{\sum_{i=1}^n (O_i - \bar{O})^2}, \quad (1)$$

$$R^2 = \frac{\left(\sum_{i=1}^n (O_i - \bar{O})(P_i - \bar{P}) \right)^2}{\sum_{i=1}^n (O_i - \bar{O})^2 \sum_{i=1}^n (P_i - \bar{P})^2}, \quad (2)$$

where n is the number of observed data, O_i and P_i are the observed and simulated values at time i , and \bar{O} and \bar{P} are the observed value and the average value of a simulation, respectively. The closer the values of the two functions are to 1, the better the simulation results of the model are. Similar to other studies^[31–32], the results of the objective function can be evaluated as poor, fair, good and very good in the model performance.

4 Results and discussion

4.1 Comparison between original and downscaled LAI

Fig. 3 presents the enhanced LAI after downscaling and shows the agreement between the original MODIS (500 m) and downscaled LAI (30 m) at the scale of the entire basin and a typical magnified view on August 20, 2008. As expected, much more detailed spatial LAI patterns can be found in the downscaled LAI but have been averaged out in the original MODIS LAI. The normalized frequency distribution (Fig. 3c) also indicates that equivalent clusters exist among the two downscaled and original LAIs.

4.2 Calibration and validation of SWAT simulations

According to sensitivity analysis, parameter calibrations for the original SWAT model and the improved SWAT model are focused on eight parameters, including CN2, ALPHA_BF, GWQMN, REVAPMN, RCHRG_DP, SOL_AWC, SOL_K and ESCO (Table 2). Note that the α coefficient of base flow (ALPHA_BF) is obtained by the base flow division of runoff data software.

Then, combined with MODIS LAI data, the original and improved SWAT models were used to simulate runoff. The validation for both simulations was based on the runoff observations at the Fenkeng hydrographic station (Fig. 4). The Nash coefficient and correlation coefficient R^2 between observations and simulations are shown in Table 3. We find that the E_{NS} and R^2 are above 0.8 in both cases, indicating that the simulations are close to the measured values. The model performance for both models can thus be evaluated as "very good". The comparison of simulations between the two models shows that the simulated runoff from the improved model has a smaller variability over the period of 2001–2014. In addition, the E_{NS} and R^2 for the improved model were higher than those in the original model during the period for parameter calibration (R^2 increases from 0.93 to 0.95 and E_{NS} increases from 0.86 to 0.93, respectively). A similar change is also evident in the validation period (R^2 increases from 0.93 to 0.95 and E_{NS} increases from 0.86 to 0.93, respectively). The model comparison results show that the robustness of the improved model is better. According to the results of previous research, the ENS was noticeably improved when the ENS increased by 0.02–0.09 and was slightly improved when the ENS increased by 0.01–0.02 (Peterson and Hamlett, 1998; Zhou et al., 2013). Therefore, the accuracy of SWAT simulation is noticeably improved after combining MODIS LAI.

4.3 Spatial and temporal distribution of green water and blue water

Blue water resources are the sum of basin water production

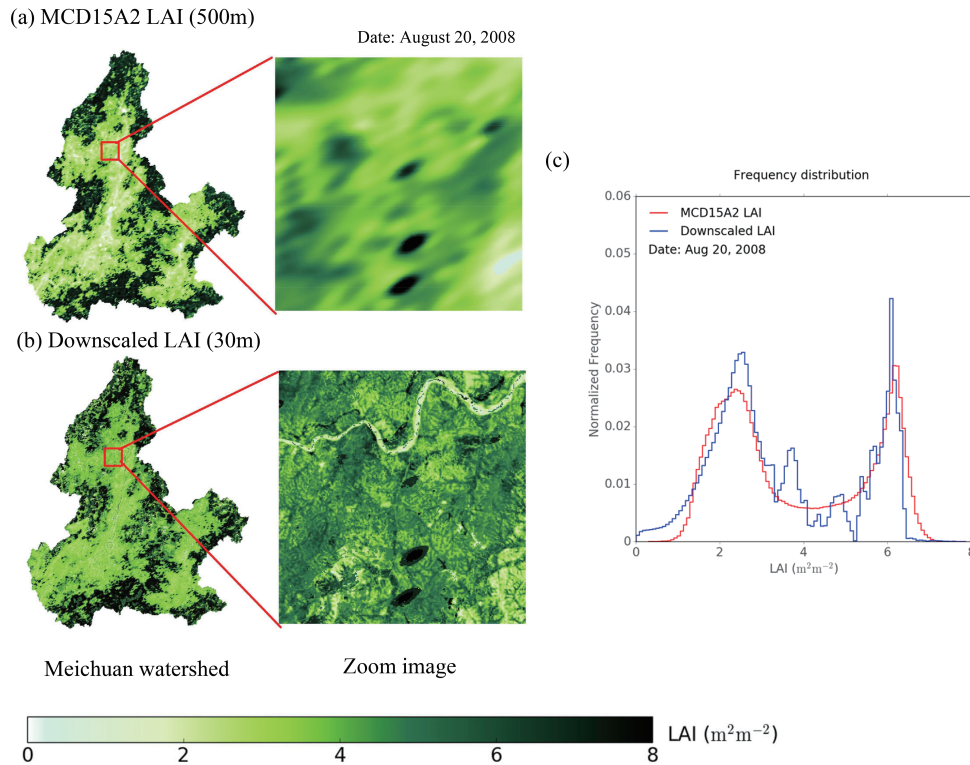


Fig. 3. MCD15A2 (a) and downscaled (b) maps of LAI on August 20, 2008. The right plot (c) shows the normalized frequency distributions of these two LAI maps.

Table 2. List of eight sensitive parameters in SWAT used to calibrate streamflow with their calibrated values.

Parameter	Definition(Unit)	Calibrated values (original/improved)
CN2	Initial SCS runoff curve number for moisture condition II	0.02/-0.03
ALPHA_BF	Baseflow alpha factor (1/day)	0.032/0.032
GWQMN	Threshold depth of water in the shallow aquifer required for return flow to occur (mm)	2643/300
REVAPMN	Threshold depth of water in the shallow aquifer for “revap” or percolation to the deep aquifer to occur (mm)	36/230
RCHRG_DP	Deep aquifer percolation fraction	0.19/0.7
SOL_AWC	Available water capacity of the soil layer (mm)	0.34/0.32
SOL_K	Saturated hydraulic conductivity(mm/hr)	0.36/0.71
ESCO	Soil evaporation compensation factor	0.84/0.06

(WYLD) and deep groundwater recharge (DA_RCHG). Green water flow is evapotranspiration (ET). Green water reserves denote soil moisture content (SW), and green water resources are equal to the sum of green water flow and green water reserves. Based on the above calculations, we can obtain the temporal variations in the overall blue water and green water resources in the Meichuan River Basin during the study period (Table 4).

As shown in Table 4, the average precipitation in the Meichuan River Basin was 1628.97 mm during the period of 2003-2014. The average total water resources of 1764.08 mm is approximately 1.8 times the annual mean amount of blue water resources (total available water). The amount of blue water resources will increase with heavy precipitation, suggesting that precipitation is the main source of blue water resource replenishment and the most influential factor of blue

water resources. The average amount of green water resources from 2003 to 2014 was 790.58 mm, accounting for 44.8% of the total water resources. The equal amount between blue water resources and green water resources reveals that green water resources play an important role in water resource contributions. Green water flow (evapotranspiration) serves as the main part of green water resources. Thus, most green water resources are lost by the evapotranspiration of vegetation. Notably, the total water resources simulated by the model are not equal to the precipitation. This difference can be attributed to inaccurate simulation of the initial soil water content in the SWAT model^[33].

Fig. 5 shows the spatial distribution of several parameters, including annual averaged precipitation, blue water resources, green water resources, and the hydrological components of water resources. The annual mean precipitation generally de-

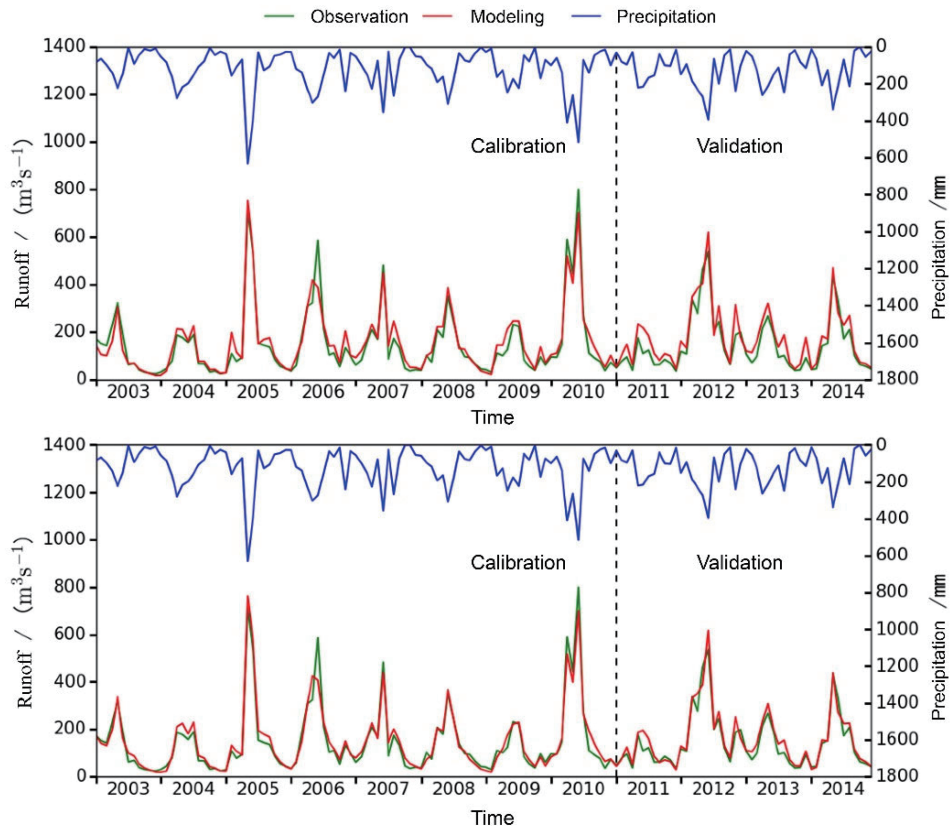


Fig. 4. Temporal variability of rainfall, observed and estimated monthly runoff from original (a) and modified (b) SWAT with MODIS LAI at Fengeng station.

Table 3. Evaluation statistics of the runoff simulated by the original and modified SWAT model.

Period	Model	Average(mm)	Maximum(mm)	Minimum(mm)	StandardDeviation	R ²	E _{NS}
Calibration	Original	181.44	860.7	19.73	157.23	0.93	0.93
	Improved	175.77	872.2	20.55	160.61	0.95	0.95
Validation	Original	203.29	706.3	48.66	140.83	0.91	0.83
	Improved	182.48	706	33.93	137.63	0.94	0.92

Table 4. Blue and green water resources (mm) in the Meichuanjiang Basin during 2003–2014.

Year	Precipitation	Total water resources	Blue water resources	Green water resources	Green water flow	Green water reserves
2003	1072.8	1392.76	722.07	670.69	638.71	31.98
2004	1438.06	1461.79	653.98	807.81	715.43	92.38
2005	1940.36	2000.57	1210.63	789.94	656.81	133.13
2006	1848.14	1920.59	1112.92	807.67	655.13	152.54
2007	1493.29	1698.73	935.06	763.67	645.69	117.98
2008	1539.35	1662.11	840.77	821.34	714.1	107.24
2009	1426.22	1514.21	669.05	845.16	679.97	165.19
2010	1989.79	2133.18	1352.84	780.34	634.05	146.29
2011	1335.71	1483.61	686.54	797.07	646.98	150.09
2012	2363.12	2353.91	1579.42	774.49	608.03	166.46
2013	1443.24	1719.74	916.1	803.64	647.53	156.11
2014	1657.56	1827.71	1002.57	825.14	695.64	129.5
Average	1628.97	1764.08	973.5	790.58	661.51	129.07

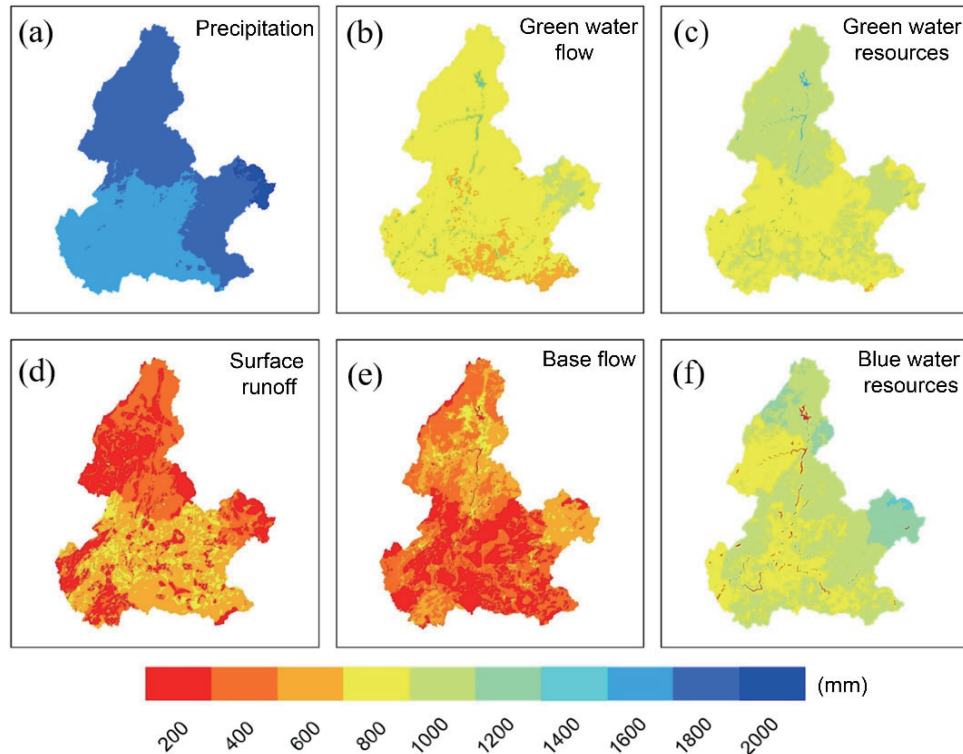


Fig. 5. Spatial distribution of annual mean water resource components in the Meichuan Basin during 2003-2014: (a) precipitation, (b) green water flow, (c) green water resources, (d) surface runoff, (e) base flow and (f) blue water resources.

increases from northeast to southwest in the study area (Fig. 5a). The surface runoff in the northern basin is lower than that in the southern basin, while the base flow has an opposite pattern. This spatial pattern is consistent with the north–south distribution of precipitation, suggesting that precipitation controls the surface runoff and base flow in the whole basin. The amount of green water resources along the river is obviously higher than that in other areas. This feature can be explained by green water resources produced by human activities. Because the crops in the southern subtropical basin were planted in the area along the river course and require more agricultural irrigation water, the increase in the overall evapotranspiration results in a larger amount of green water resources along the river course. In addition, the green water resources in the northern part of the basin are higher than those in the southern part. For green water flow, there is no obvious change in the basin.

4.4 Changes in blue and green water resources before and after the improvement of the SWAT model

By comparing the simulated blue and green water resources before and after the improvement of the SWAT model (Fig. 6), it is found that the blue water resources from the improved SWAT model increase by 86.41 mm and the green water resources decrease by 37.80 mm. This change is related to the following two reasons. First, the remote sensing LAI used in the plant growth module of the improved SWAT is lower than that simulated by the original model, resulting in a decrease in evapotranspiration and green water resources. Second, a smaller proportion of rainfall infiltrated and retained the soil, which increased the amount of runoff (blue wa-

ter). For each component of blue and green water resources, we found an increase in base discharge surface and green water reserves, with a decrease in runoff and green water discharge. In comparison, the change in green water flow and base flow is more significant because changes in vegetation directly affect the amount of evapotranspiration (green water flow) and rainfall infiltration. In addition, the Meichuan River Basin is located in a humid area with a relatively high surface vegetation coverage rate. This leads to an increase in the proportion of the green water flow and the base flow.

For the spatial distribution, the green water flow simulated by the improved SWAT model is lower, and green water reserves become higher than simulations before the model improvement (Fig. 6). The changes in green water resources show an obvious difference between the northern and southern regions of the basin due to the difference in vegetation types. The major vegetation type in the south is forest, while the major vegetation types in the north are farmland, grassland and shrub. Thus, low LAI values are shown in the northern region, with a greater reduction in evapotranspiration (green water flow). Another reason for spatial differences is associated with the strong ability of forests to conserve water and soil. In forest regions, rainfall can be converted into soil water storage even if the LAI is reduced, and thus, the increase in soil water (green water reserves) is more significant.

In Fig. 7, the variation trend of blue water resources is opposite to that of green water resources. Compared with the original model, the blue water resources simulated by the improved model increase significantly with a level of approximately 120–270 mm. The main reason is that the reduction in vegetation increases the conversion rate of rainfall to runoff

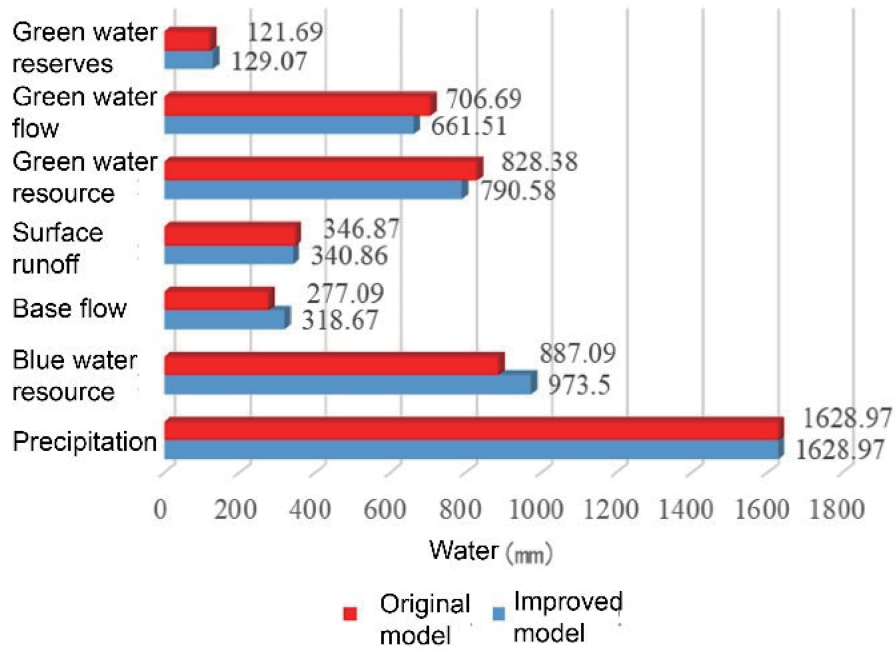


Fig. 6. Estimated components of water resources from the original and modified SWAT models during 2003–2014.

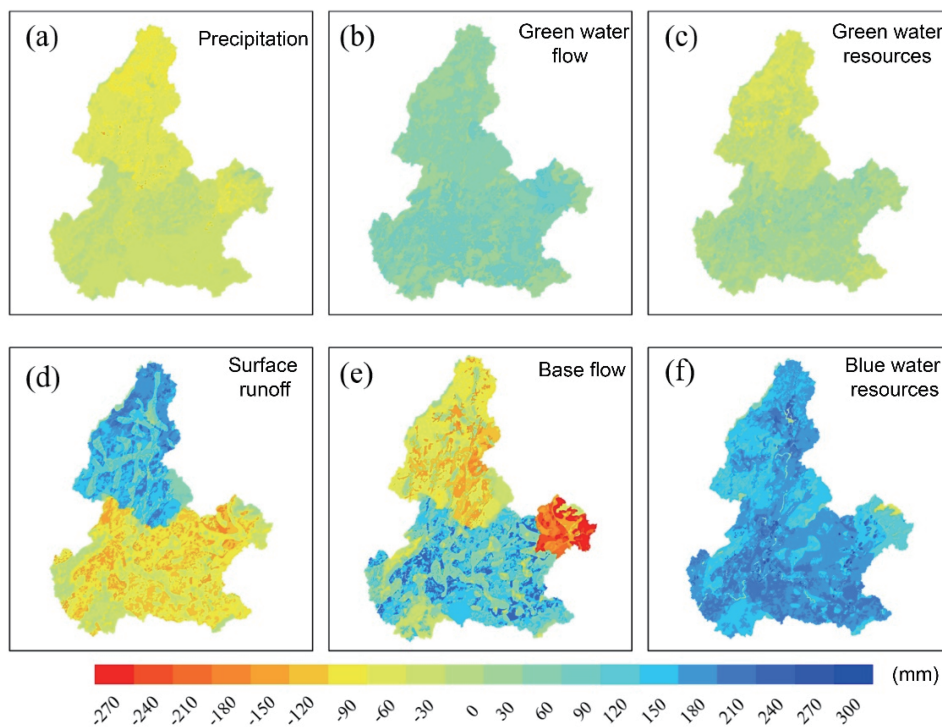


Fig. 7. Comparison of blue and green water resource components between the original and modified SWAT models during 2003–2014.

(blue water). Two main components of blue water resources, i.e., surface runoff and base flow, vary significantly from north to south. The surface runoff increases and the base flow decreases in the northern region, while an opposite trend is shown in the southern region. Similar to the north–south difference in green water resource distribution, different changes in blue water resources occur in response to vegetation types. For farmland, grassland and shrub, vegetation reduction leads

to a small roughness coefficient, accelerates the velocity of overland flow, and thus results in a decrease in the infiltration of water during the runoff process. Correspondingly, there is a significant increase in surface runoff and a decrease in base flow. For forests, a large proportion of infiltrated rainfall can be converted into base flow. Therefore, surface runoff will decrease when vegetation cover and forest interception of rainfall decrease in the basin. In addition, the analysis

of soil spatial distribution and hydrometeorological conditions shows that the change in soil and surface runoff and the change in precipitation and base discharge play an important role.

4.5 Impact of vegetation change on estimation of blue and green water resources

Fig. 8 shows the estimation of blue and green water resources in response to vegetation change before and after model improvement. For the green water resources of farming land, grassland and shrub, their estimated values with the improved model decrease more in autumn and winter than in spring and summer. In contrast, the green water of the three forest vegetation types had no obvious change at the seasonal scale. Based on the analysis in Section 4.3 and 4.4, we have learned that evapotranspiration is the dominant component of green water resources. Thus, the decrease in green water resources in autumn and winter is due to the decrease in evapotranspiration induced by vegetation reduction. However, the changes in evapotranspiration cannot explain the decrease in green water resources in spring and summer. Although the vegetation cover rate in spring and summer is higher than that in autumn and winter, the reduced evapotranspiration is lower than that in autumn and winter. It can be concluded that the reason for the reduction in green water in spring and summer is that the decrease in vegetation cover leads to an increase in solar radiation received by the surface and a decrease in soil water content.

The simulations from the improved model show that the blue water resources of grassland and shrub have a greater increase, with annual average rates of 21.5% and 19.7%, respectively, followed by farmland and deciduous forest, with change rates of 18.9% and 18.2%, respectively. The change rates of evergreen forest and mixed forest were the lowest at 10.8% and 11%, respectively. The blue water resources increase with LAI changes and vegetation reduction. This also implies that vegetation has a significant water-reducing effect and can conversely increase the water and soil conservation ability in the basin.

The changes in blue and green water resources of forests

before and after the model improvement indicate that the seasonal change in vegetation has negligible effects on the change in blue and green water resources for forests. The main reason is that the short-term vegetation reduction associated with the small change in evapotranspiration has little effect on the change in overall water balance, especially for forests with large evapotranspiration. In addition, forests have a better water and soil conservation ability. This will cause the increase in blue water sources and the decrease in green water sources to be nonsignificant.

To further understand the relationship between vegetation change and water sources, we compare the LAI time series obtained from the original model with that from the improved model. As shown in Fig. 9, the LAI simulated by the original model is relatively high. This comparison is consistent with the changes in green water resources between the original and modified SWAT models (Fig. 7), indicating that green water is mainly affected by vegetation change. The LAI simulated by the original model peaked quickly and occupied a long time in the vegetation growth cycle, while there was no such phenomenon in the simulations of the improved model. We could not obtain an appropriate LAI curve that reasonably describes vegetation dynamics as the MODIS LAI presented even though the SWAT parameters had been adjusted to keep plant growth at the slowest speed. This could be attributed to the EPIC model used in SWAT, which is only adaptable to a temperate zone (Alemayehu et al., 2017).

Temperature is the most important controlling factor governing plant growth in EPIC. In temperate zones, the temperature when seeding is approximately 10~15 °C and rises to 30~35 °C 2~3 months before harvesting (Bai et al., 2018). Considering the plant growth pattern in the temperate zone, the accumulation of heat units is slow, especially at the beginning of plant growth (Neitsch et al., 2011). However, there is an extremely rapid accumulation of heat units in the tropics and subtropics due to high temperatures throughout the whole year, resulting in an incredible rapid LAI increase at the beginning of the growing season in SWAT-EPIC. In addition, previous studies have demonstrated that the nature of vegeta-

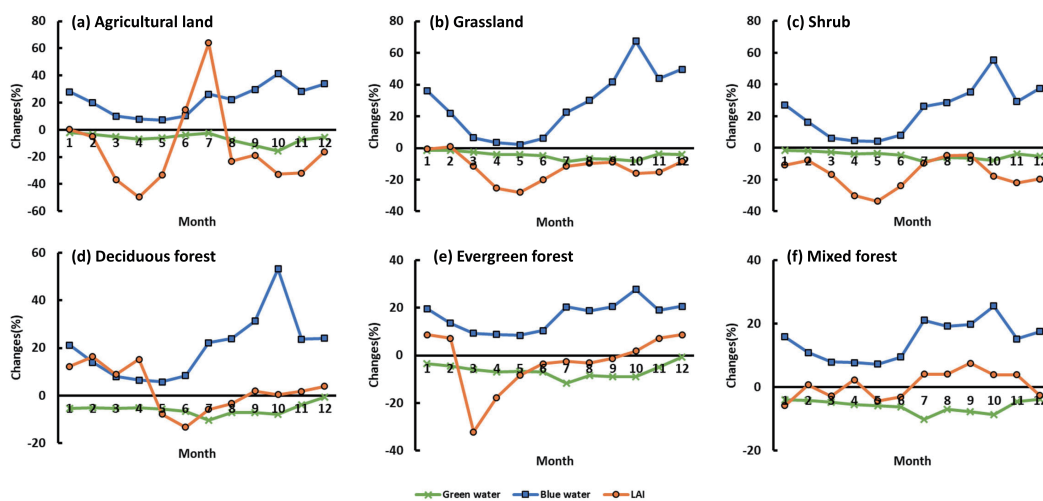


Fig. 8. Simulated monthly changes (%) in rainfall, LAI, blue and green water resources in the Meichuan Basin by original and modified SWAT models.

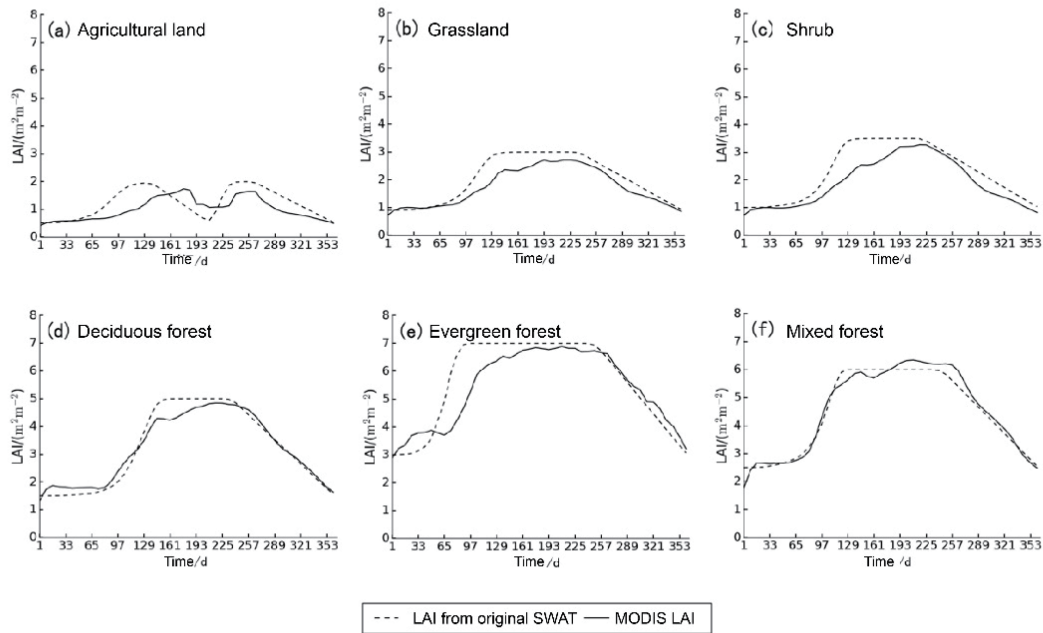


Fig. 9. The time series of LAI as simulated by the original SWAT and modified SWAT with MODIS LAI.

tion growth in the subtropics is controlled by rainfall, not temperature (Ma et al., 2019). Therefore, the modeled LAI values were abnormally higher than the observed satellite values in all vegetation types. All of the above issues were also the reason why we tried to use satellite-observed LAI to replace the SWAT-simulated LAI.

5 Conclusions

In this study, remote sensing LAI was processed by scale conversion and then incorporated into the SWAT model. The modified SWAT can thus be applied in tropical and subtropical regions, and its simulations also show a relatively high accuracy in the studied area. Meanwhile, the comparison between the blue water and green water resources estimated by the original model and the modified model reveals the important influence of vegetation change on the spatial and temporal change distribution pattern of blue water and green water resources. Because the LAI can affect evapotranspiration, green water is more sensitive to vegetation change than blue water. The estimates of the improved model for the green water resources are higher and the blue water becomes lower, and they are closer to the actual changes. Changes in vegetation can cause the change in blue water and green water amount in agricultural grassland to be more significant than that in forestland. The forest has a good conservation and regulation capacity, and thus, its seasonal change has no obvious effect on the change in blue and green water. In the process of improving SWAT, this study uses MODIS 500 m/8 days LAI remote sensing products that have been published steadily for a long time and do not require additional correction for field observations or specific satellite data processing. Thus, data preparation and processing are very simple. This improved model is a useful tool for the accurate and comprehensive evaluation of water resource effects and the ecological environment.

Acknowledgments

This work was supported by the National Natural Science Foundation of China (42206242), Open Research Fund of State Key Laboratory of Simulation and Regulation of Water Cycle in River Basin (China Institute of Water Resources and Hydropower Research, No. IWHR-SKL-KF202303), the State Key Laboratory of Cryospheric Science for the Open fund (SKLCS 2020-06), the Fundamental Research Funds for the Central Universities (WK2080000161), and the Nature Science Research Project of Anhui Province (2108085QD158).

Conflict of interest

The authors declare that they have no conflicts of interest.

Biographies

Tianming Ma is currently a postdoctoral fellow at the School of Earth and Space Sciences, University of Science and Technology of China. He received his Ph.D. degree in Marine Science from Tongji University in 2020. His research mainly focuses on ice core studies and paleoclimate.

Tianxiao Ma is currently an assistant research fellow at the Institute of Applied Ecology, Chinese Academy of Sciences. He received his Ph.D. degree in Geographic Information and Systems from the University of Chinese Academy of Sciences in 2019. His research mainly focuses on landscape ecology.

References

- [1] Zhen T, Xu Z, Cheng L, et al. Spatiotemporal distributions of blue and green water resources: A case study on the Lushi watershed. *Resources Science*, **2010**, 32 (6): 1177–1183. (in Chinese)
- [2] Falkenmark M. Land and Water Integration and River Basin Management. Rome, Italy: FAO, **1995**.
- [3] Rost S, Gerten D, Bondeau A, et al. Agricultural green and blue water consumption and its influence on the global water system.

- Water Resources Research*, **2008**, *44* (9): W09405.
- [4] Liu J, Wang Y, Yu Z, et al. A comprehensive analysis of blue water scarcity from the production, consumption, and water transfer perspectives. *Ecological Indicators*, **2017**, *72*: 870–880.
- [5] Falkenmark M, Rockström J. The new blue and green water paradigm: Breaking new ground for water resources planning and management. *Journal of Water Resources Planning & Management*, **2006**, *132* (3): 129–132.
- [6] Xu J. Increasing trend of green water coefficient in the middle Yellow River basin and the eco-environmental implications. *Acta Ecologica Sinica*, **2015**, *35* (22): 7298–7307.
- [7] Veetil A V, Mishra A K. Water security assessment using blue and green water footprint concepts. *Journal of Hydrology*, **2016**, *542*: 589–602.
- [8] Badou D F, Diekrüger B, Kapangaziwiri E, et al. Modelling blue and green water availability under climate change in the Beninese Basin of the Niger River Basin, West Africa. *Hydrological Processes*, **2018**, *32* (16): 2526–2542.
- [9] He X, Wang G, Bao Z. Progress and prospective of climate and vegetation coverage change as well as responses of hydrological cycle. *Journal of Water Resources and Water Engineering*, **2016**, *27* (2): 1–5.
- [10] Yang D, Lei H, Cong Z. Overview of the research status in interaction between hydrological processes and vegetation in catchment. *Journal of Hydraulic Engineering*, **2008**, *39* (Z2): 1142–1149.
- [11] Liu J, Gao G, Wang S, et al. The effects of vegetation on runoff and soil loss: Multidimensional structure analysis and scale characteristics. *Journal of Geographical Sciences*, **2018**, *28* (1): 59–78.
- [12] Zhao A, Zhao Y, Liu X, et al. Impact of human activities and climate variability on green and blue water resources in the Weihe River Basin of Northwest China. *Scientia Geographica Sinica*, **2016**, *36* (4): 571–579.
- [13] Du L, Rajib A, Merwade V. Large scale spatially explicit modeling of blue and green water dynamics in a temperate mid-latitude basin. *Journal of Hydrology*, **2018**, *562*: 84–102.
- [14] Tadesse A, Ann V G, Tadesse W B, et al. An improved SWAT vegetation growth module and its evaluation for four tropical ecosystems. *Hydrology and Earth System Sciences*, **2017**, *21* (9): 4449–4467.
- [15] Strauch M, Volk M. SWAT plant growth modification for improved modeling of perennial vegetation in the tropics. *Ecological Modelling*, **2013**, *269* (1771): 98–112.
- [16] Kiniry J R, Macdonald J D, Kemanian A, et al. Plant growth simulation for landscape-scale hydrological modelling. *International Association of Scientific Hydrology*, **2008**, *53* (5): 1030–1042.
- [17] Arnold J G, Kiniry J R, Srinivasan R, et al. Soil and water assessment tool input/output file documentation: Version 2009. Temple, TX: Texas Water Resources Institute, **2011**: No. 365.
- [18] Ma T, Duan Z, Li R, et al. Enhancing SWAT with remotely sensed LAI for improved modelling of ecohydrological process in subtropics. *Journal of Hydrology*, **2019**, *570*: 802–815.
- [19] Wagner P D, Kumar S, Fiener P, et al. Hydrological modeling with SWAT in a monsoon-driven environment: experience from the Western Ghats, India. *Transactions of the ASABE*, **2011**, *54* (5): 1783–1790.
- [20] Lamparter G, Nobrega R L B, Kovacs K, et al. Modelling hydrological impacts of agricultural expansion in two macro-catchments in Southern Amazonia, Brazil. *Regional Environmental Change*, **2018**, *18* (1): 91–103.
- [21] Lai G, Qiu L, Zhang Z, et al. Modification and efficiency of SWAT model based on multi-plant growth mode. *Journal of Lake Sciences*, **2018**, *30* (2): 472–487.
- [22] Huang M, Ji J. The spatial-temporal distribution of leaf area index in China: A comparison between ecosystem modeling and remote sensing reversion. *Acta Ecologica Sinica*, **2010**, *30* (11): 3057–3064. (in Chinese)
- [23] Xiao Z, Wang J, Wang Z. Improvement of MODIS LAI product in China. *Journal of Remote Sensing*, **2008**, *12* (6): 993–1000. (in Chinese)
- [24] Zhang H, Gao W, Shi R. Reconstruction of high-quality LAI time-series product based on long-term historical database. *Journal of Remote Sensing*, **2012**, *16* (5): 986–999. (in Chinese)
- [25] Yuan H, Dai Y, Xiao Z, et al. Reprocessing the MODIS Leaf Area Index products for land surface and climate modelling. *Remote Sensing of Environment*, **2011**, *115* (5): 1171–1187.
- [26] Li R, Zhu A, Li B, et al. Response of simulated stream flow to soil data spatial detail across different routing areas. *Process in Geography*, **2011**, *30* (1): 80–86. (in Chinese)
- [27] Emelyanova I V, Mcvicar T R, Van Niel T G, et al. Assessing the accuracy of blending Landsat–MODIS surface reflectances in two landscapes with contrasting spatial and temporal dynamics: A framework for algorithm selection. *Remote Sensing of Environment*, **2013**, *133* (12): 193–209.
- [28] Houborg R, McCabe M F, Gao F. A Spatio-Temporal Enhancement Method for medium resolution LAI (STEM-LAI). *International Journal of Applied Earth Observation and Geoinformation*, **2016**, *47*: 15–29.
- [29] Abbaspour K C, Rouholahnejad E, Vaghefi S, et al. A continental-scale hydrology and water quality model for Europe: Calibration and uncertainty of a high-resolution large-scale SWAT model. *Journal of Hydrology*, **2015**, *524*: 733–752.
- [30] Zhao K, Su B, Shen M, et al. An improved method for parameter identification of SWAT model. *South-to-North Water Transfers and Water Science & Technology*, **2017**, *15* (4): 49–53.
- [31] Luo K, Tao F. Hydrological modeling based on SWAT in arid northwest China: A case study in Linze County. *Acta Ecologica Sinica*, **2018**, *38* (23): 8593–8603.
- [32] Nan Z, Zhao Y, Li S. Improvement of snowmelt implementation in the SWAT hydrologic model. *Acta Ecologica Sinica*, **2013**, *33* (21): 6992–7001.
- [33] Moriasi D N, Arnold J G, Liew M W V, et al. Model evaluation guidelines for systematic quantification of accuracy in watershed simulations. *Transactions of the ASABE*, **2007**, *50* (3): 885–900.